NANO LETTERS

2005
Vol. 5, No. 5
853−857

Local Electronic Structure of Single-Walled Carbon Nanotubes from Electrostatic Force Microscopy

Jinseong Heo and Marc Bockrath*

Department of Applied Physics, California Institute of Technology, M/C 128-95, Pasadena, California 91125

Received January 27, 2005; Revised Manuscript Received April 13, 2005

ABSTRACT

An atomic force microscope was used to locally perturb and detect the charge density in carbon nanotubes. Changing the tip voltage varied the Fermi level in the nanotube. The local charge density increased abruptly whenever the Fermi level was swept through a van Hove singularity in the density of states, thereby coupling the cantilever's mechanical oscillations to the nanotube's local electronic properties. By using our technique to measure the local band gap of an intratube quantum-well structure, created by a nonuniform uniaxial strain, we have estimated the nanotube chiral angle. Our technique does not require attached electrodes or a specialized substrate, yielding a unique high-resolution spectroscopic tool that facilitates the comparison between local electronic structure of nanomaterials and further transport, optical, or sensing experiments.

Atomic force microscopy (AFM) is a widely employed technique for sensing small forces. While it has been used extensively to image the structure of materials on nanometer or even atomic scales,[1] relatively little work has been done employing AFM to probe the *electronic* properties of materials. We report a technique by which the local electronic properties of single-walled carbon nanotubes (SWNTs) are coupled to an AFM cantilever's mechanical motion by using electrostatic force microscopy (EFM)[2−4] to sense electrostatic forces between an AFM tip and the nanotubes. EFM has previously shown promise as a probe of the local density of states (LDOS) by probing the electron system in Bi nanowires.[5] Our technique, unlike previous studies, utilizes a convenient and flexible sample geometry, does not require attached electrodes, and provides a calibrated energy scale, thus enabling the LDOS to be probed spectroscopically with nanometer-scale resolution. This permits the results of transport, optical, or sensing experiments and applications to be compared with detailed information about local electronic structure.

We exploit the relationship between the charge density in an electron system and its Fermi level, which reflects its fundamental properties. Measurements of electronic compressibility, which is determined by this relationship, have been used to study electron−electron interactions in two-dimensional electron systems,[6] investigate the metal−insulator transition,[7] and identify fractional localized charges in quantum Hall systems.[8] In our experiment, we populate the nanotubes' one-dimensional (1D) subbands by varying the tip voltage. The resulting variations in the compressibility of the electron gas modulate the tip−sample capacitance, causing the van Hove singularities in the density of states to be reflected in the electrostatic forces acting on the cantilever. Our results demonstrate the effects of quantum confinement on a nanotube's capacitance, which may have important implications for the high-frequency operation of nanotube devices.[9] Moreover, we have exploited this capability to measure the local band gap of an intratube quantum-well structure, created by the application of a nonuniform uniaxial strain.[10] From the local band gap versus the local strain, we infer the nanotube chiral angle by comparison to theoretical models.[11−13] The technique is applicable to other materials and should find wide applicability in investigating the properties of nanoscale systems.

A degenerately doped silicon wafer capped with a 1 μm oxide layer supports single-walled carbon nanotubes (SWNTs) grown by chemical vapor deposition.[14] A Si atomic force microscope cantilever with an integrated tip vibrates near its resonant frequency and scans over the sample surface to probe the SWNTs. After acquiring topographical height using tapping mode, the tip then makes a second pass over each line, at a larger height Δh relative to the sample. With careful adjustment of Δh, during the lowest point of oscillation the tip−sample separation becomes less than a few nm. During each second pass the tip is biased at voltage V; the phase shift $\Delta\phi$ between the mechanical drive and the cantilever's motion is recorded. Once a nanotube is located, the slow

* Corresponding author. E-mail: mwb@caltech.edu.

10.1021/nl0501765 CCC: $30.25
Published on Web 04/29/2005

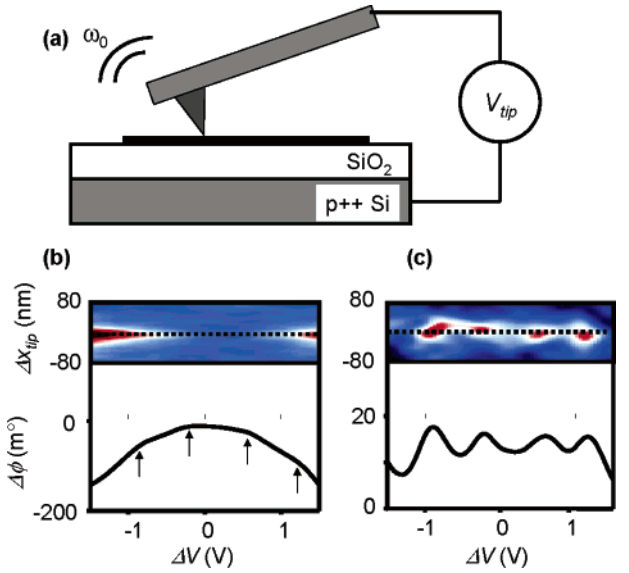

Figure 1. Experimental geometry and cantilever response to electrostatic forces (a) A vibrating cantilever with free amplitude A is brought close to a nanotube supported by an oxidized Si wafer. In the topographic scan, feedback maintains the amplitude at a reduced value of A_{tap}. (b) Upper panel: color plot of $\Delta\phi$ vs Δx and voltage $\Delta V = V - V_{min}$, where V_{min} (typically $\sim$ 1 V) corresponds to a maximum in $\Delta\phi$ obtained with $\Delta h = 30$ nm, $A \sim$ 150 nm, $A_{tap} \sim 100$ nm. The data are smoothed over a $\sim$10 pixel radius. Dark red corresponds to -150 m° while dark blue corresponds to 0.0 m°. The dotted line indicates the nanotube position. Lower panel: $\Delta\phi$ vs ΔV when the tip is directly above the nanotube. Arrows mark kinks in $\Delta\phi$ vs ΔV. (c) upper panel: color plot of $\Delta\phi$ vs Δx and ΔV with a smooth background subtracted. Dark red corresponds to 20 m° while dark blue corresponds to 5 m°. When the tip is directly over the nanotube, the data show peaks in $\Delta\phi$ vs ΔV. Lower panel: $\Delta\phi$ vs ΔV taken along the dotted line exhibiting a series of peaks. The voltages giving the peaks correspond to the voltages yielding the kinks in the data of part (b).

scan axis is disabled so the tip retraces the same nominal line over the nanotube. This setup is illustrated in Figure 1a. The nanotube grounded either by its capacitance to the ground plane, or by attached electrodes.[15] V is incremented at the end of each scan line. As V varies, electrostatic forces acting on the cantilever's tip change its effective spring constant, modulating $\Delta\phi$. The upper panel of Figure 1b shows a color scale plot of $\Delta\phi$ vs ΔV and tip position Δx for a 0.9 nm diameter SWNT, where ΔV includes an offset to account for tip−sample work function differences. The dashed line indicates the nanotube position. The lower panel of Figure 1b shows a line trace of $\Delta\phi$ vs ΔV when the tip is directly over the nanotube.

The line trace approximately follows the trend $\Delta\phi \propto -\Delta V^2$, as reported and elucidated in previous studies[15,16] but with notable differences. Remarkably, $\Delta\phi$ shows kinks at the voltages indicated by the arrows. Subtracting a smooth background from the data in Figure 1b yields the data in Figure 1c, which is approximately proportional to $-d^2(\Delta\phi)/dV^2$ and enhances the contrast of these features. The upper panel shows the background-subtracted $\Delta\phi$ vs Δx and ΔV in a color scale. When the tip is directly over the nanotube, $\Delta\phi$ shows a series of peaks as ΔV varies. These peaks occur

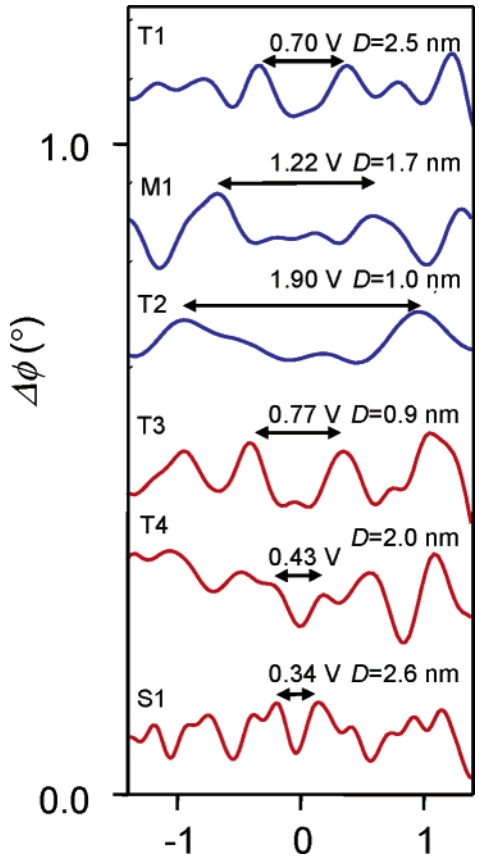

Figure 2. Background subtracted $\Delta\phi$ vs ΔV for six nanotube samples T1−T4, S1 and M1. S1 and M1 were determined by transport measurements to be semiconducting and metallic, respectively, while no electrodes were attached to T1−T4. The peaks are offset horizontally slightly to align the minima, and offset vertically for clarity. To obtain a consistent vertical scale, the data have been scaled by a multiplicative factor for each tube. The scale factors for each sample are T1, ×10; T2, ×4; S1, ×0.5; T3, ×10; M1, ×0.6; T4, ×6. Data from T1−T4 were taken with $\Delta h = \sim$30 nm, $A \sim$ 150 nm, $A_{tap} \sim$ 100 nm, while data from S1 and M1 was taken with $\Delta h = 7$ nm, $A \sim 30$ nm, $A_{tap} \sim 15$ nm. The combination of smaller A and Δh typically gives larger peaks in $\Delta\phi$ vs ΔV, as reflected by the smaller scale factors for S1 and M1. The voltage gap V_g between peaks surrounding $\Delta V = 0$ is indicated, along with the diameter D for each tube. V_g depends on the nanotube diameter. For a given diameter, the data from samples with relatively small V_g are shown in red, and those with a large V_g are shown in blue.

at the same voltage positions of the kinks shown in Figure 1b. The line trace shown in the lower panel shows peaks at $\Delta V = -0.2$ V and $\Delta V = 0.7$ V, as well as two additional peaks near $\Delta V \sim \pm 1$ V.

The voltage position of the peaks is nanotube-dependent. Figure 2 shows $\Delta\phi$ vs ΔV for six different nanotubes, labeled T1−T4, S1, and M1. Transport measurements were performed on S1 and M1. S1 was determined from these measurements to be semiconducting, while M1 was determined to be metallic. For each tube, a gap region near $\Delta V = 0$ is surrounded by peaks of typical width $\sim$150 mV, with additional peaks at larger $|\Delta V|$.[17] Arrows delineate the voltage gap V_g and the measured nanotube diameter D is given.

To understand this behavior, we consider cantilever's motion in the presence of electrostatic forces. In the simplest picture, the electrostatic force gradient changes the effective

spring constant, modulating $\Delta\phi$. The force gradient is proportional to d^2C_{ts}/dz^2, where C_{ts} is the tip−sample capacitance and z the mean tip height. However, C_{ts} should reflect contributions both from the geometric capacitance C as well a quantum capacitance $C_Q = e^2n^2\kappa L$ in series with C, where $\kappa = n^{-2}dn/d\mu$ is the electron gas compressibility, n the carrier density, L is the characteristic length of the tip−sample capacitor, e is the electric charge, and μ is the chemical potential (e.g., ref 18). This series addition of C_Q to C accounts approximately for the kinetic, exchange and correlation energy of the electrons. From recent ab initio calculations[19] we expect C_Q makes an appreciable contribution to the C_{ts} for a nanotube, regardless of L, originating from nanotubes quasi-1D nature.

For μ such that electrons just begin to occupy each additional subband, the 1D density of states has a van Hove singularity. C_Q then becomes large, and the induced charge on the nanotube will increase more rapidly with ΔV. A quantitative calculation, however, of $\Delta\phi$ vs ΔV requires numerical computations, since the forces acting on the tip are strongly anharmonic. Nevertheless, the abrupt increase in induced charge when the Fermi level is at a 1D van Hove singularity should produce kinks in $\Delta\phi$ vs ΔV, as observed. Upon subtracting a smooth background these kinks will yield peaks.

For metallic nanotubes, the energy separation between the van Hove singularities near the Fermi level is $eV_g[\text{eV}] \approx 2.16\ D^{-1}\ [\text{nm}^{-1}]$, based on semiempirical calculations used successfully to interpret previous STM studies[20] (e.g., ref 21). ΔV is related to μ by $d\mu/e = C/(C+C_Q)\ d\Delta V$ For these tubes, the voltage separation between successive peaks is then 2.16 V D^{-1} [nm^{-1}] $(C_Q + C)/C$. For semiconducting nanotubes when μ is in the band gap, the electron gas is incompressible and μ/e and ΔV are related in a 1:1 ratio. The band gap E_g then determines the voltage spacing between peaks, giving $V_g[\text{V}] = E_g/e \approx 0.72\ D^{-1}\ [\text{nm}^{-1}]$.[21]

Plotting eV_g vs D^{-1} in Figure 3 shows that eV_g generally increases with increasing D^{-1}, with most of the data falling on one of two clusters corresponding to eV_g differing by a factor of 3 for a given diameter. The open triangles show data from tubes without attached electrodes. The solid squares show eV_g vs D^{-1} for semiconducting nanotubes (as determined from transport experiments), which fall in the lower cluster. Accordingly, all tubes with eV_g falling on the lower line are inferred to be semiconducting. The expected relation between eV_g and D^{-1} for semiconducting nanotubes is plotted as the lower solid line in Figure 3. The data indicated by squares and lower four open triangles follow this line very closely. We emphasize that *the lower line has no free parameters*.

The upper data set taken from the metallic nanotubes also follows a straight line. Fitting a line to obtain the slope gives $(C_Q + C/C) \approx 1.0$. The three remaining points marked by open triangles also fall near this upper line. Remarkably, this implies that $C \gg C_Q$ for metallic nanotubes, and $d\mu/e \approx d\Delta V$. We estimate C as $C = 2\pi\epsilon\epsilon_0/\ln(s/d)\ L$, where ϵ is the dielectric constant, ϵ_0 is the permittivity of free space, s is the tip-tube separation, and d is the tube diameter. Taking

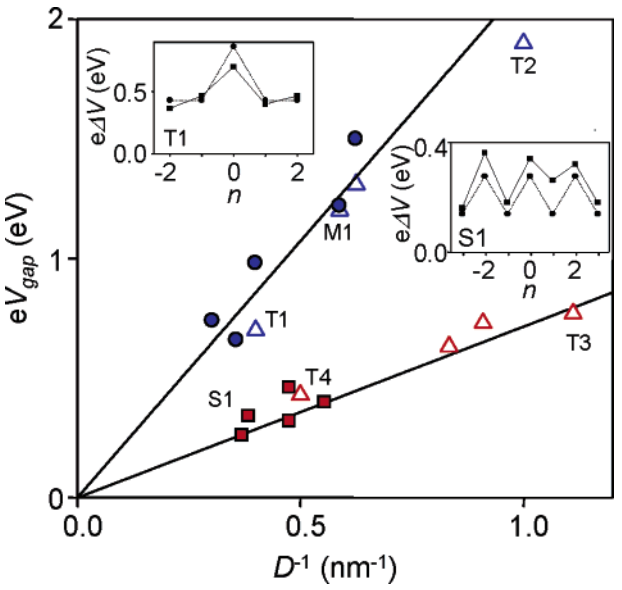

Figure 3. Plot of eV_g vs D^{-1}. Transport experiments were performed on some nanotubes to determine whether they were semiconducting or metallic. The squares show data from semiconducting nanotubes, falling on the lower line. The circles show data from metallic nanotubes, falling on the upper line. The upper line is a fit to the metallic tube data with a slope of 2.16 eV nm. The lower line is a line with a slope of 0.72 eV nm, plotted without free parameters. Open triangles denote eV_{gap} vs D^{-1} for eight samples that did not have attached electrodes. The left inset shows filled squares connected by solid lines denoting intervals between peaks for sample T1. The filled circles joined by dashed lines show the theoretical expectation. Right inset, filled squares connected by solid lines denote intervals between peaks for sample S1. The filled circles joined by dashed lines show the theoretical expectation.

$\epsilon\sim1$, $s\sim2$ nm, and $d\sim1$ nm, $C\sim8\times10^{-17}$ F $L[\mu\text{m}] < C_Q$. However, this estimate neglects the presence of the water capillary that forms under ambient conditions between the tip and sample when their separation is less than a few nm, as occurs in our experiment.[22−26] Since water's dielectric constant is ~80, it can strongly modify C_{ts} during the lowest part of the cantilever oscillation cycle when it approaches the surface and the capillary forms. With $\epsilon\sim80$, the previous estimate yields instead $C\sim6\times10^{-15}$ F $L[\mu\text{m}]$. Thus we expect to find features in $\Delta\phi$ vs ΔV consistent with $C \gg C_Q$ and $d\mu/e \approx d\Delta V$, in agreement with the relation obtained from a fit to the data for metallic nanotubes.

This inference is further supported by periodic patterns of peak positions in ΔV. For some nanotubes, particularly those with $D >$ ~2 nm, the peak arrangement in ΔV depends on whether they are metallic or semiconducting. For semiconducting tubes, the peaks cluster in groups of two, alternating between large intervals $\delta(\Delta V)\sim V_g$ and small intervals $\delta(\Delta V) \sim V_g/2$, as exemplified by S1. These intervals are plotted in the right inset to Figure 3 by filled squares. For metallic (or small band gap) tubes, there is one large interval of $\delta(\Delta V)=V_{gm}$ near $\Delta V = 0$, with the other intervals $\delta(\Delta V) \sim V_{gm}/2$, as exemplified by T1. Filled squares in the left inset to Figure 3 denote these intervals from T1. These patterns are readily accounted for by using a low-energy model, which is expected to be accurate for nanotubes in the given size range.[27] In this picture, the energy spacing

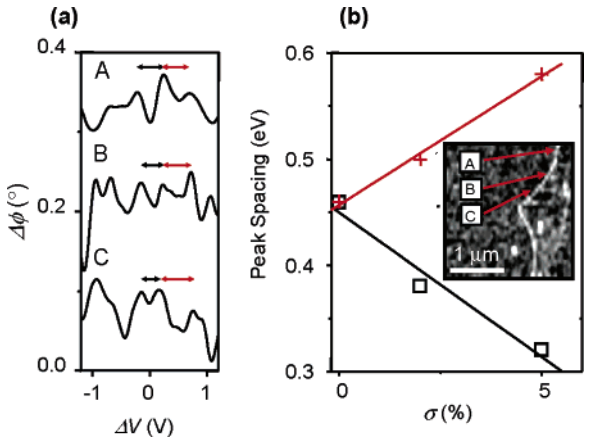

Figure 4. Effect of nanotube strain on van Hove singularity positions. (a) Plot of $\Delta\phi$ vs ΔV for a strained nanotube taken at the positions A, B, and C indicated in the inset to part (b). Curves are offset for clarity. The arrows indicate two successive peak intervals for data taken from each location. Size of gap and measured tube diameter indicate that this tube is semiconducting. (b) Band gap (open squares) and second interval (crosses) vs estimated local strain.

between successive van Hove singularities in semiconducting nanotubes is expected to alternate between E_g and $E_g/2$, while metallic nanotubes are expected to have one large interval E_{gm}, with the rest equal intervals of $E_{gm}/2$, consistent with our observations. The expected intervals, assuming $d\mu/e \approx d\Delta V$, are plotted as filled circles connected by dashed lines in Figure 3 for S1 in the right inset and for T1 in the left inset, using only the measured diameter of the nanotubes as the input parameter. These calculated intervals are in good agreement with the data.

This picture of meniscus formation and the resulting large geometric capacitance obtained accounts qualitatively for the peaks' presence, and quantitatively for the voltage gap V_g for both metallic and semiconducting nanotubes *without free parameters*. Taken together, this demonstrates that atomic force microscopy can be used to probe the local density of states in nanotubes, yielding a spectroscopic technique in which μ is directly tuned by V to yield a calibrated energy scale.

To further demonstrate the capabilities of our technique, we measured the local band gap of an artificially produced quantum well structure within a semiconducting nanotube. Longitudinal strain has been shown both theoretically[13,28,29] and experimentally[11,12] to modulate the band structure of nanotubes. Figure 4 shows an AFM image of a nanotube pushed by an AFM tip to make a stretched region. We then probed the LDOS at the points labeled A, B, and C. Point A is outside of the displaced region and yields an energy gap of 0.45 eV. This is consistent with the expectation for the band gap of semiconducting nanotube with the measured diameter $D = 1.9$ nm of 0.38 eV. From the shape of the tube, we estimate the local strain at point B and C to be ~2% and ~5% respectively.[10] We note these estimates are only approximate, since the assumption that the strain is concentrated only in the displaced region may be oversimplified.[30]

Figure 4b shows eV_g vs σ in the lower data set. We observe the shifting of van Hove singularities at chemical potentials further away from the Fermi level for a neutral tube. The upper set of data in Figure 4b shows the energy gap between the first and second van Hove singularities eV_{g1}. Fitting a straight line to the measured eV_g vs σ shows that the band gap diminishes by $dE_g/d\sigma \sim 24$ meV/% of strain, while eV_{g1} increases by ~27 meV/% of strain. This is in qualitative agreement with theoretical predictions, which predict equal and opposite energy shifts for these gaps under strain. Quantitatively, $dE_g/d\sigma$ is expected to be ≈100 meV $\cos(3\theta)$, where θ is the chiral angle of the nanotube. $\theta = 0°$ for a zigzag nanotube, and $\theta = 30°$ for an armchair tube.[13] The chiral angle of the nanotube exhibited in Figure 4 is then be estimated as ~$1/3 \cos^{-1}$(24 meV/100 meV) ~ 25°.

The decrease of the band gap with strain constrains the chiral indices for a (n,m) nanotube to satisfy $n - m = 3q - 1$, where n,m and q are integers. This constraint, coupled with careful measurements of diameter and the strain-dependence of the gap, could enable the determination of the chiral indices for a given nanotube using only electrostatic forces and mechanical strain. Comparison of the present data with that of micro-Raman studies will be helpful in this regard and may help to ascertain the numerical accuracy of the theory of ref 13.

In conclusion, we have demonstrated that AFM can be used to probe the electronic density of states in carbon nanotubes and distinguish individual metallic and semiconducting nanotubes without using attached electrodes. This capability should prove useful in efforts to control nanotube synthesis or separation to yield selected electronic properties. Finally, unlike scanning tunneling microscopy, our measurements can be readily performed on insulating substrates. Future work should enable detailed images of the local electronic structure of nanotubes or other nanomaterials to be directly compared to the results of further transport, optical or sensing experiments.

Acknowledgment. We thank C. N. Lau for helpful discussions. Supported by Arrowhead Research Corporation and the Charles Lee Powell Foundation.

References

(1) Quate, C. F. *Surf. Sci.* **1994**, *299*, 980.
(2) Stern, J. E.; Terris, B. D.; Mamin, H. J.; Rugar, D. *Appl. Phys. Lett.* **1988**, *53*, 2717.
(3) Schönenberger, C.; Alvarado, S. F. *Phys. Rev. Lett.* **1990**, *65*, 3162.
(4) Martin, Y.; Abraham, D. W.; Wickramasinghe, H. K. *Appl. Phys. Lett.* **1988**, *52*, 1103.
(5) Gekhtman, D.; Zhang, Z. B.; Adderton, D.; Dresselhaus, M. S.; Dresselhaus, G. *Phys. Rev. Lett.* **1999**, *82*, 3887.
(6) Eisenstein, J. P.; Pfeiffer, L. N.; West, K. W. *Phys. Rev. Lett.* **1992**, *68*, 674.
(7) Ilani, S.; Yacoby, A.; Mahalu, D.; Shtrikman, H. *Science* **2001**, *292*, 1354.
(8) Martin, J.; Ilani, S.; Verdene, B.; Smet, J.; Umansky, V.; Mahalu, D.; Schuh, D.; Abstreiter, G.; Yacoby, A. *Science* **2004**, *305*, 980.
(9) Li, S. D.; Yu, Z.; Yen, S. F.; Tang, W. C.; Burke, P. J. *Nano Lett.* **2004**, *4*, 753.
(10) Bozovic, D.; Bockrath, M.; Hafner, J. H.; Lieber, C. M.; Park, H.; Tinkham, M. *Phys. Rev. B* **2003**, *67*, 033407.
(11) Minot, E. D.; Yaish, Y.; Sazonova, V.; Park, J. Y.; Brink, M.; McEuen, P. L. *Phys. Rev. Lett.* **2003**, *90*, 156401.

(12) Cao, J.; Wang, Q.; Dai, H. J. *Phys. Rev. Lett.* **2003**, *90*, 157601.
(13) Yang, L.; Han, J. *Phys. Rev. Lett.* **2000**, *85*, 154.
(14) Kong, J.; Soh, H. T.; Cassell, A. M.; Quate, C. F.; Dai, H. *Nature* **1998**, *395*, 878.
(15) Bockrath, M.; Markovic, N.; Sheppard, A.; Gurevich, L.; Kouwenhoven, L.; Wu, M.; Sohn, L. *Nano Lett.* **2002**, 2, 187.
(16) Bachtold, A.; Fuhrer, M.; Plyasunov, S.; Forero, M.; Anderson, E. H.; Zettl, A.; McEuen, P. L. *Phys. Rev. Lett.* **2000**, *84*, 6082.
(17) The small features that occur within the gap region in M1 and features of similar relative magnitude in the other data are likely noise, as determined by comparing their magnitude to the noise background found when the tip was away from the nanotubes.
(18) Buttiker, M. *J. Phys. Condens. Mater.* **1993**, *5*, 9361.
(19) Pomorski, P.; Pastewka, L.; Roland, C.; Guo, H.; Wang, J. *Phys. Rev. B* **2004**, *69*, 115418.
(20) While small band gap nanotubes have van Hove singularities at typical energy scales $E_{gs} \sim 30$ meV, the small effective mass leads to reduced spectral weight of these singularities and additionally, thermal smearing prevents their observation since $k_B T \sim E_{gs}$. Therefore, we expect small band gap tubes to have a similar observable van Hove singularity spacing as metallic tubes.
(21) Kim, P.; Odom, T. W.; Huang, J. L.; Lieber, C. M. *Phys. Rev. Lett.* **1999**, *82*, 1225.
(22) Piner, R. D.; Zhu, J.; Xu, F.; Hong, S.; Mirkin, C. A. *Science* **1999**, *283*, 661.
(23) Xu, L.; Lio, A.; Hu, J.; Ogletree, D. F.; Salmeron, M. *J. Phys. Chem. B* **1998**, *102*, 540.
(24) Zitzler, L.; Herminghaus, S.; Mugele, F. *Phys. Rev. B* **2002**, *66*, 155436.
(25) Colchero, J.; Storch, A.; Luna, M.; Herrero, J. G.; Baro, A. M. *Langmuir* **1998**, *14*, 2230.
(26) Beaglehole, D.; Christenson, H. K. *J. Phys. Chem.* **1992**, *96*, 3395.
(27) Kane, C. L.; Mele, E. J. *Phys. Rev. Lett.* **1997**, *78*, 1932.
(28) Heyd, R.; Charlier, A.; McRae, E. *Phys. Rev. B* **1997**, *55*, 6820.
(29) Yang, L.; Anantram, M. P.; Han, J.; Lu, J. P. *Phys. Rev. B* **1999**, *60*, 13874.
(30) Cronin, S. B.; Swan, A. K.; Ünlü, M. S.; Goldberg, B. B.; Dresselhaus, M. S.; Tinkham, M. *Phys. Rev. Lett.* **2004**, *93*, 167401.

NL0501765